Design considerations for the integration of energy harvesting systems with energy-aware task schedulers

Leonardo Kessler Slongo*[1], Arliones Hoeller Jr[2], Antônio Augusto Fröhlich[3], and Eduardo Augusto Bezerra[4]

[1,2,3]Software/Hardware Integration Lab (LISHA) - Technology Center - Federal University of Santa Catarina - Postal Code 88040900 - Florianópolis - Santa Catarina - PO Box 476

Phone/Fax: +55-48-3721-9516

[4]Embedded Systems Group (GSE) - Technology Center - Federal University of Santa Catarina - Postal Code 88040900 - Florianópolis - Santa Catarina - Phone: +55-48-3721-2358 - Fax: +55-48-3721-9280

[1]leokessler@lisha.ufsc.br, [2]arliones@lisha.ufsc.br, [3]guto@lisha.ufsc.br, [4]eduardo.bezerra@eel.ufsc.br

Abstract

This work presents a solar energy harvesting circuit envisioned to extend the lifetime of low power wireless sensing platforms. The energy harvesting circuit operates solar panels closely to their maximum power point only by precisely matching them to the batteries. The circuit improves an energy-aware, wireless sensor network system by providing the task scheduler with more frequent and accurate measurements of battery charge. The paper discusses the circuit design and evaluation, and shows its capability for extending systems' lifetime. A simulation evaluates the proposed system, showing that the task scheduler was able to run all critical tasks, while also running 1.23 times more non-critical tasks when compared to the previous approach. Finally, the outdoor tests allowed an experimental correlation between the current delivered by the solar panels and the solar irradiance, which will be used for including environmental prediction capability on the energy-aware schedulers.

Keywords: Solar energy harvesting, energy-aware task scheduler, low power wireless platforms, solar panel, wireless sensor networks.

I. INTRODUCTION

Energy consumption is a determining factor when designing wireless sensor networks. As a consequence, battery lifetime is a limitation on the development of such systems. Therefore, the idea of extracting energy from the environment has become attractive. Looking to the energy consumption problem, the intelligent usage of the stored energy contributes to extend the sensor nodes' longevity. Consequently, energy schedulers have been developed in order to adequately assess the energy consumption and adapt the system accordingly to the available amount of energy. The purpose of this work is to adapt a solar energy harvesting circuit to supply energy to low power wireless platforms, i.e., those that operate under 50mW. Simultaneously, we aim at improving the performance of the energy-aware task scheduler in wireless sensor network systems by providing fine-grained battery and environmental monitoring.

Among a number of energy sources that have been studied so far, solar has proved to be one of the most effective[1]. The solar energy conversion through photovoltaic (PV) cells is better performed at an optimum operating voltage. Operating a solar panel on this voltage results in transferring to the system the maximum amount of power available. In this context, *maximum power point tracker circuits* (MPPT) have been proposed. The drawback is that MPPT circuitry may introduce losses to a solar harvesting system. Concerning low-power applications, it may be more energy efficient to have a good matching between the solar panel and the energy storage unit[2]. This well matched system is than able to work close to the maximum power point with less power loss.

In this work, an evaluation of the proposed harvesting circuit is performed in order to show improvements on an energy-aware task scheduler[3]. It is shown that the combination of the proposed circuit with the cited scheduler not only extended the longevity of the wireless sensor network, but also improved system quality.

The paper is organized as follows: Section II presents the fundamentals of solar energy harvesting and energy-aware task scheduler. Section III discusses the design of the harvesting circuit under the perspective of low power wireless platforms. Section IV presents the evaluation of the harvesting circuit and a case study showing the improvements on system quality. Finally, section V closes the paper.

II. FUNDAMENTALS

Energy-aware task scheduling has been a subject of intense research for the last three decades. Specifically for wireless sensor network systems, energy-aware issues have been investigated from a design-time perspective, mainly in four fronts: low-power hardware design[4]; low-power communication protocols[5,6] ; low-power applications[7]; and efficient energy sources[8]. A little effort has been dedicated to optimize the system performance through task scheduling while reducing energy cost in wireless sensor networks[9].

In this paper, we build on previous research[3] in order to identify the benefits of having a more precise way of monitoring the energy source on real-time wireless sensor network systems. We specifically focus on wireless sensor networks systems that harvest energy from solar irradiation through photovoltaic cells. Within this context, this section describes a few fundamentals of the used technologies.

A. Solar Energy

Power management is one of the main research topics in wireless sensor networks. Batteries, which have a limited energy capacity, are the most common option for powering sensors. Sleeping modes and low power communication protocols[10] emerged as a solution to extend systems' lifetime. Although this allows a better distribution of the consumed energy along the network, the idea of energy harvesting has been applied in order to deliver more energy to the nodes. This implies on further enhancement of system quality, as volume of communication and processing may be raised proportionally to the amount of available energy.

Table I: Power Densities of Harvesting Technologies

As Table I shows, different harvesting technologies present different power densities[1]. Also, it is shown that the solar modality presents the highest power density. However, many parameters should be taken into account when planning to operate a photovoltaic module, including solar irradiance, temperature variation, mechanical position and the photovoltaic module's electrical characteristics. Through experimentation, photovoltaic cells' characteristic power and current curves, like the ones in Figure 1, are obtained under known operating parameters (e.g. temperature of 25^{o}C and an irradiance of 1000W/m^{2}).

Figure 1: Typical solar cell voltage-current and voltage-power curves of polycrystalline silicon cells.

These curves demonstrate that solar cells are remarkably versatile as they can operate from the state of open circuit -- where, theoretically, there is no current flowing -- to the state of short circuit -- where, theoretically, there is no voltage drop between the positive and negative terminals of the solar cell. The solar cell power curve is nothing but the product of voltage and current values in *y* and *x* axis. With this concept in mind, and assuming positive values for voltage and current, the power curve must have at least one maximum value. In order to extract the maximum power of the environment, a solar panel must operate as close as possible to this maximum power point. Normally, the maximum power is extracted from the solar panel by applying to it the V_{MPP} (voltage at maximum power point). Electronic circuits, called *maximum power point trackers* (MPPT), are responsible for ensuring the operation on this point.

The idea of operating a solar panel as close as possible to its V_{MPP} is not new[11]. The microelectronic industry has already developed integrated circuits able to keep a solar panel operating on its V_{MPP}. Most of these IC's, however, are dedicated to high power applications and present high power consumption, making it generally incompatible with low-power energy harvesting systems. Hence, MPPT circuits for low power applications are also being investigated. These circuits operate by detecting changes on the solar panel, computing the new V_{MPP} and applying this voltage to the photovoltaic module. Changes in the behavior of the photovoltaic module happen mainly due to variations in temperature and solar irradiance. Thus, sensors are needed to monitor state changes. As these sensors imply in extra load in the system, its use also is often unfeasible in energy-sensitive or low-power systems.

In order to solve this problem, electronic circuits were developed to extract the solar cell information directly from its electrical characteristics. Methods as Perturb and Observe[12,13], Incremental Conductance[14,15], Fractional Open Circuit Voltage[16,17], Constant Voltage[18] are the most known. Although these are interesting methods, the solution described here is focused on working as close as possible to the MPP through an ideal match between the battery and the photovoltaic module. Although it is not the most efficient method, it is the simplest way of operating a solar panel closely to its MPP, and its efficiency have already been proved[2]. Besides its simplicity, this circuit provides accurate battery information to the sensing platform, what drove a significant improvement in its structure.

B. Energy Consumption Monitoring

Since this work is strongly related with the energy consumption of the sensing platform, it is convenient to elucidate the currently implemented method for estimating its energy consumption and how it can be improved. The current method, *Battery Level Monitoring by Event Accounting*[3], proposes the energy consumption model described by Equations 1 through 3 to estimate the battery charge.

$$E_{tm}(dev) = (t_{end} - t_{begin}) \cdot (I_{dev,mode}) \quad (1)$$

$$E_{ev}(dev) = \sum_{event\ counters} E_i \cdot counter \quad (2)$$

$$E_{tot}(dev) = E_{tm}(dev) + E_{ev}(dev) \quad (3)$$

The idea is to estimate the energy consumed by the devices in the sensing platform through two different perspectives. The first one (Equation 1) is dedicated to devices (*dev*) operating with constant current (*I*) over a time period (*t*) and in a determined mode (*mode*). The second perspective (Equation 2) is event-based (e.g., sensor sampling), where energy consumed by specific events (E_i) are accumulated periodically according to the number of accounted events (*counter*). Finally, this total energy consumption (Equation 3) is defined by the sum of $E_{tm}(dev)$ and $E_{ev}(dev)$.

Components' datasheets are the base to estimate the inputs for equations 1 and 2 ($I_{dev,mode}$ and E_i). Therefore, those equations render a pessimistic but safe estimation. In order to avoid underestimations when considering the worst case, the system measures battery voltage periodically to estimate actual battery charge. The battery energy (E_{batt}) is then calculated as shown in Equation 4, where E_{volt} is the battery energy estimation based on the battery voltage reading.

$$E_{batt} = max\left(E_{volt}, E_{batt} - \sum_{i=0}^{devs} E_{tot}(i)\right) \quad (4)$$

Measuring the battery voltage through a shunt resistor is the drawback of this method due to its power loss. This results in sporadic measurements. Besides providing the sensing platform with an energy

harvesting circuit, the work in this paper also contributes to the performance of the scheduling mechanism. The performance enhancement is achieved by replacing E_{volt} by the energy consumption readings of the battery monitor IC, which are more accurate. Also, the measurement may be realized with a higher frequency in the new approach, since these measurements are supported by the power coming from the solar panels.

III. DESIGN CONSIDERATIONS

This section explains how the proposed solar harvesting circuit was designed. It presents a reasoning about technical decisions and modifications implemented on the Heliomote project[2], in order to support motes based on low power wireless platforms. Finally, the performance of the harvesting circuit is evaluated through outdoor experiments.

A. Solar Cell and Energy Storage Unit

The relation between the solar cell and the energy storage unit is a crucial issue for the proposed harvesting circuit. This highlights the need of working as close as possible to the MPP, in order to extract the maximum amount of energy available. Since the circuit has no maximum power point tracker (the solar cells are directly coupled to the battery), the battery operating voltage should be as close as possible to the V_{MPP} for the selected solar cell.

The two available technologies to store energy, in a rechargeable way, are batteries and super capacitors. Although super capacitors are improving, they are not recommended for solar harvesting circuits yet due to intrinsic leakage, losses on parasitic paths in the external circuitry[2], and low energy density. Among all the battery technologies available (e.g., Sealed Lead Acid, Nickel Cadmium, Nickel Metal Hydride, Lithium based), the Nickel Metal Hydride (NiMH) was chosen mainly for the low complexity on the recharging circuit and the absence of memory effect. Consequently, the system is powered by two common AA NiMH batteries with a nominal charge capacity of *2100mA*.

The PV module is composed by two *4V-100mA* solar cells measuring *60x60mm*. The solar cell's characterization curves were plotted (Figures 2 and 3) based on data collected outdoor, on March 08, 2012 at 1:15 pm, with an average irradiance of $954W/m^2$. The goal of the test was to find out the open circuit voltage (V_{OC}), the short circuit current (I_{SC}) and the V_{MPP} in a real scenario. Table II shows the

obtained values.

Figure 2: Solar panel characterization carried outside - current-voltage curve.

Figure 3: Solar panel characterization carried outside - power-voltage curve.

Table II: Solar Panel Measured Parameters

B. Adaptation for an Low Power Wireless Platform

In order to understand the adaptations proposed for low power wireless platforms, it is essential to know some of their characteristics. Table III shows three different examples that have motivated the changes applied to Helimote's circuit. They are typical Platform-in-Package (PiP) which features a *2.4GHz* radio frequency transceiver. As shown in Table III, all these PiPs may operate with voltages lower than *3.3V*. Therefore, there is no need for the step-up converter used in Heliomote's project. The new generation of PiPs normally operates at *1.8V*, having a built-in buck regulator. Hence, the harvesting circuit efficiency is improved by eliminating the step-up converter.

Table III: Wireless MCU's Electrical Characteristics

C. Circuit Design

The harvesting circuit is planned to charge the NiMH batteries until a predefined threshold voltage. This voltage is set by external resistors in a voltage monitor (ICL7665). The threshold voltage selected was based on the charging behavior of the NiMH battery provided by the manufacturer (see Figure 4). This battery is considered fully charged when it reaches a voltage around *1.45V* (*0.1C* curve). The selected threshold voltage was *2.9V*, since the two AA cells were aranged in-serie. An analog switch short circuits the solar panel to ground when this value is reached. The overvoltage signal provided by the ICL7665 controls the analog switch. This prevents battery overcharges. A normally opened (MAX4614) analog switch were used instead of a normally closed one. Hence, if the initial battery voltage is bellow *2V* it is charged by the solar panel instead of being short circuited to the ground as in the case of using a normally closed one.

Figure 4: Charging curves for AA Nickel Metal Hidryde battery[19].

The circuit must also take care of the undercharge situation. There are two different reasons to avoid that. First, there is a minimum voltage threshold from which batteries do not operate properly. In this case,

it is recommended to disconnect the load in order to avoid battery degradation. The second reason is that the input voltage of the wireless MCU's should not be lower than *2V*. Thus, the under voltage pin of the ICL7665 is connected to a transistor. Then, when the battery voltage drops below *2.1V* the transistor is opened, disconnecting the mote. A simplified block diagram of the harvesting circuit is shown in Figure 5.

Besides the already mentioned features, the circuit has a battery monitor (DS2438). This IC communicates trhough a protocol called 1-Wire. It provides the battery's information (battery voltage, battery current, remaining capacity and temperature) that may be used by a energy-aware task scheduler. The DS2438 also has an integrated current accumulator, which informs the total current going in and out of the battery.

Figure 5: Simplified block diagram of a sensing platform solar harvesting circuit.

IV. CASE STUDY: SCHEDULING IN MOBILE WSN

The proposed approach was integrated to the power management mechanism of EPOS[20]. EPOS is a component-based operating system for embedded applications. Also, we ran this implementation in the EPOSMoteII platform[21], a module for the development of low-power wireless sensor network applications. Hardware evaluation was performed by analysis of data in an actual implementation. The scheduling approach was evaluated by means of simulation taking the characterization of the mentioned platform into consideration. The remaining of this section describes the setup of the evaluation scenario and the obtained results.

A. EPOSMoteII Solar Energy Harvesting Circuit

In order to adequately characterize the developed circuit integrated to the EPOSMoteII sensing platform, an outdoor test was performed. The test period was 62 hours and 45 minutes. For the test, the EPOSMoteII radio was configured to constantly transmit random data. This 100% duty cycle was used in order to test critical conditions and also to reduce test duration. By reducing the duty cycle, it would be necessary to extend the test to several weeks, since the total current consumption when the system is in standby mode is only around *5μA*, i.e., more than 5,000 times smaller than the *29mA* it consumes when transmitting data at full power.

Figure 6 shows the battery voltage behavior during the test. In all recharge cycles, the battery has

almost reached the fully recharged voltage. However, there are differences among the peak values, which shows that the maximum voltage reduced from one peak to the previous one. This fact is explained analyzing the amount of energy delivered by the battery. Figure 7 shows that the system has lost energy after each cycle, which means that, for a 100% duty cycle, this system would not be self-sufficient.

Figure 6: Battery voltage behavior.

Figure 7: Energy evolution.

The test started on March 16, 2012 at 9:15 pm, i.e. during night, what explains why the first descending slope in Figure 7 is shorter than the other two. Current integration was used in order to calculate the energy expended on slopes. The first complete slope spent *738.43mAh*, while the second spent *746.96mAh*. The small difference between these values is justified by the difference on the daylight duration, which, although similar, was not perfectly equal in both days. The analysis of these values is of paramount importance when selecting the capacity of the storage unit. This extreme case (100% duty cycle) helps to justify the need for an energy-aware scheduler in the system. The descending slopes must be reduced in order to have a self-sufficient system.

Figure 8 shows the current delivered by the solar panel, which was calculated by subtracting the system's current (considered constant at *56mA* due to the constant duty cycle) from the input/output battery current. Figure 9 shows the solar irradiance acquired during the test by a pyranometer placed close to the system's photovoltaic panel at the same inclination (27°). The current delivered by the solar panel and the solar irradiance were plotted in order to obtain an equation to correlate them. This curve and its linear approximation are shown in Figure 10. This plot is an additional contribution of this work, since it is through this linear equation (Equation 5, where I_{panel} is the current delivered by the solar panel in *mA* and *Irrad* is the solar irradiance in W/m^2) that the energy-aware task scheduler may forecast energy input. This plot will motivate the development of new heuristics for the scheduler which will further improve its efficiency.

Figure 8: Current delivered by the solar panel.

Figure 9: Solar irradiance variation.

Figure 10: Relation between current and solar irradiance.

$$I_{panel} = 0.20628 \cdot Irrad \quad (5)$$

Solar irradiance and delivered current present a linear behavior when variations in temperature are not taken into consideration. Figure 11 adds temperature variation, which is the main reason for the spread points in Figure 10. A new mathematical model considering temperature variation is being developed in order to design an energy-aware task scheduler with more precise environmental prediction.

Figure 11: Temperature variation.

B. Evaluation Scenario

The application used to evaluate the approach is a mobility-enabled wireless sensor network. This network runs the Ant-based Dynamic Hop Optimization Protocol (ADHOP) over an IP network using IEEE 802.15.4. ADHOP is a self-configuring, reactive routing protocol designed with the typical limitations of sensor nodes in mind, energy in particular[22]. ADHOP's reactive component relies on an *Ant Colony Optimization* algorithm to discover and maintain routes. Ants are sent out to track routes, leaving a trail of pheromone on their way back. Routes with a higher pheromone deposit are preferred for data exchange.

EPOS scheduler relies on EPOS power manager to adaptively run the system. In EPOS adaptive task scheduling model, tasks are classified as hard real-time or best-effort. In order to guarantee system lifetime, EPOS energy scheduler reserves the amount of energy the system will need to run hard real-time tasks until a desired lifetime is reached. Best-effort tasks are only allowed to execute when excess energy exists. In EPOS scheduler, different heuristics can be used to control system quality degradation when best-effort tasks are prevented from executing. Once specific heuristics for managing energy consumption are not the focus of the present work, only EPOS global energy allocation heuristic was considered[3].

The objective of this case study is to demonstrate how the employment of the proposed energy input measurement mechanism enhanced system performance. Thus, ADHOP had to be modified. ADHOP's tasks have then been classified as hard real-time or best-effort. The main idea behind this setup was to homogenize the battery discharge for every node in the network to enhance the lifetime of the network as a whole. Considering the radio the most energy-hungry component in a wireless sensing node, we made

the design decision of modeling the routing activity of ADHOP as a best-effort task, as shown by the task set at Table IV. The basic node functionality of sensing a value (task *Sense*) and forwarding it through the radio to the next node (task *Forward*) where modeled as hard real-time tasks. The functionality of forwarding other nodes' packets (and ants) when acting as a “router” was modeled as two best-effort tasks, one for monitoring the channel for arriving messages (*LPL* - Low Power Listen), and another to effectively receive the message and route it to another node (*Route*).

Table IV: ADHOP Case-study Tasks' Parameters

The simulation time, was set to 25 days. By analyzing the task set, it is possible to compute the total energy consumption of hard real-time tasks for the desired lifetime to be of *602mAh*. As a consequence, the initial battery charge for the system has to be greater than that to allow the system to reserve energy for the critical part of the application. The battery capacity specified

for this experiment is an of-the-shelf CR-2/3V battery with a total capacity of *850mAh*.

The simulation was performed in two steps. In the first step, a simulation using the OMNET++ Simulator characterized the application’s response to variations in the execution rate of best-effort tasks (BET rate). As can be seen in Figures 12 and 13, lower energy consumption at lower BET rates comes at the cost of lower data delivery rate. Also, it is possible to observe in the graphic that BET rates above 50% have no significant impact on packet delivery. Thus, it is assumed that BET rate will only be adjusted within the range [0; 50] as a means to further save energy.

Figure 12: Data delivery response to BET rate.

Figure 13: Average power and energy consumption response to BET rate.

In the second simulation step, the energy consumption of the system was simulated for 25 days, the target lifetime. As can be seen in Figure 14, the employment of the measurement mechanisms proposed here enhanced the BET rate. This happens because the proposed approach allows for more frequent adaptations that reduces the pessimistic bias of the used scheduler. It is also possible to observe that the new approach shows a better recover after relatively long periods of low irradiation, such as the one found between days 7 and 11 in Figure 15. Short periods of low irradiation, like the one on day 19, are better supported by the new approach. This can be observed by the slight decrease on BET rate on day

19 for the original method, while the new method is still reaching 50%. Over the 25-days period, 32:93% of the best-effort tasks were executed using the new approach, against 26:81% of BET rate of the former approach. This meas a total gain of 1:23 times.

Figure 14: Average BET rate over 25 days of execution using with and without the proposed approach.

Figure 15: Daily irradiation levels used for simulation.

V. CONCLUSION

Energy constraints drives the whole process of designing wireless sensor network systems. Although the use of solar energy harvesting techniques in the field have emerged along last years, only a few of them were designed for recent low power wireless platforms. Therefore, this work presented a reformulation of a solar energy harvesting circuit in order to supply energy to those platforms efficiently. Tests were carried outdoor in order to evaluate the proposed energy harvesting circuit. This circuit also allowed accurate and frequent battery charge measurements to be provided to an energy-aware task scheduler. Simulations have shown that 1.23 times more noncritical tasks were executed deploying the new harvesting circuit. Finally, the tests allowed an experimental correlation between the solar panel's current and the solar irradiance. Ongoing work is relying on this correlation to include heuristics to the energy-scheduler that may take environmental predictions into account.

ACKNOWLEDGEMENTS

This work is based in part on research funded by the CNPq (National Council for Scientific and Technological Development).

REFERENCES

[1] S. Roundy, Ph.D. dissertation, UC Berkeley, **(2003)**

[2] V. Raghunathan, A. Kansal, J. Hsu, J. Friedman, and M. Srivastava, IPSN, Los Angeles, CA, USA, pp. 457-462, **(2005)**

[3] A. H. Jr. and A. A. Fröhlich, IEEESMC, AK, USA, pp. 2608–2613 **(2011)**

[4] J. Polastre, R. Szewczyk, and D. Culler, IPSN Los Angeles, CA, USA, pp. 364-36, **(2005)**

[5] P. Huang, L. Xiao, S. Soltani, M. Mutka, and N. Xi, Communications Surveys and Tutorials, IEEE, Vol.

PP, no. 99, pp. 1-20, **(2012)**

[6] N. Pantazis, S. Nikolidakis, and D. Vergados, Communications Surveys and Tutorials, IEEE, Vol. PP, no. 99, pp. 1-41, **(2012)**

[7] L. Mottola and G. P. Picco, ACM Comput. Surv., vol. 43, no. 19, pp. 1-51, **(2011)**

[8] V. Sharma, U. Mukherji, V. Joseph, and S. Gupta, IEEE Trans. Wireless Comm., Vol. 9, no. 4, pp. 1326-1336, **(2010)**

[9] R. Kulkarni, A. Förster, and G. Venayagamoorthy, Communications Surveys and Tutorials, IEEE, Vol. 13, no. 1, pp. 68-96, **(2011)**

[10] V. Raghunathan, S. Ganeriwal, and M. Srivastava, Communications Magazine, IEEE, Vol. 44, no. 4, pp. 108-114, **(2006)**

[11] J. Schoeman and J. van Wyk, PESC, pp. 361-367, **(1982)**

[12] X. Liu and L. Lopes, PESC, Aachen, Germany, pp. 2005-2010, **(2004)**

[13] C. W. Tan, T. Green, and C. Hernandez-Aramburo, PECon, Johor Bahru, Malaysia. pp. 237-242, **(2008)**

[14] S. Jain and V. Agarwal, Power Electronics Letters., IEEE, Vol. 2, no. 1, pp. 16-19, **(2004)**

[15] S. Qin, M. Wang, T. Chen, and X. Yao, ICECE, Yichang, China, pp. 5792-5795, **(2011)**

[16] J. Ahmad, ICSTE, Puerto Rico, Vol. 1, pp. 247-250, **(2010)**

[17] D. Dondi, A. Bertacchini, L. Larcher, P. Pavan, D. Brunelli, and L. Benini, ICSET, Kathmandu, Nepal, pp. 945-949, **(2008)**

[18] G. Yu, Y. Jung, J. Choi, I. Choy, J. Song, and G. Kim, IEEE Photovoltaic Specialists Conference, pp. 1531-1534, **(2002)**

[19] Panasonic, Nickel metal hydride handbook, **(2000)**

[20] A. A. Fröhlich, International Journal of Distributed Sensor Networks, Vol. 2011, no. 1, p. 19, **(2011)**

[21] LISHA, Epos project website, [Online]. Available: http://epos.lisha.ufsc.br, **(2012)**

[22] A. M. Okazaki and A. A. Fröhlich, Joint Workshop of SCPA and SaCoNAS, IEEE GLOBECOM, Huston, Texas, USA, pp. 1179-1183, **(2011)**

Table I – Power Densities of Harvesting Technologies

Harvesting technology	Power density
Solar cells (outdoors at noon)	15 mW/cm^2
Piezoelectric (shoe inserts)	330 $\mu W/cm^3$
Vibration (small microwave oven)	116 $\mu W/cm^3$
Thermoelectric (10°C gradient)	40 $\mu W/cm^3$
Acoustic noise	330 nW/cm^3

Table II – Solar Panel Measured Parameters

Parameter	Measured Value
V_{OC}	4.15 V
I_{SC}	122.3 mA
V_{MPP}	3.25 V

Table III – Wireless MCU's Electrical Characteristics

Model	Manufacturer	Voltage	Consumption*
MC1322	Freescale	2 V – 3.6 V	29 mA
STM32W	Texas Instruments	2 V – 3.6 V	29 mA
CC2530	STMicroeletronics	2.1 V – 3.6 V	31 mA

* Current drain in transmit mode.

Table IV - ADHOP Case-study Tasks' Parameters*

Task	Period	WCET	WCEC	25-days
Sense	1,000	2	10.584	22.86
Forward	1,000	50	268.056	579.00
Collect**	5	$45.3 \cdot 10^{-6}$	$4.156 \cdot 10^{-6}$	$1.79 \cdot 10^{-3}$
LPL	5	0.25	$1.111 \cdot 10^{-6}$	$480 \cdot 10^{-6}$
Route***	50	100	490.278	21,180
Energy consumption of hard real-time tasks				601.86

* Period in ms; WCET: worst-case execution time in ms; WCEC: worst case energy consumption in nAh; 25-days: energy consumption for the targeted lifetime (25 days) in mAh.

** This is a worst-case scenario as values of "P" and, as consequence, "25-days", may change due to adaptation.

***"Route" is a sporadic task. Once it is a best-effort task in the system, we consider a hypothetic frequency of 2 Hz (period of 500 ms) to show the impact of routing in the node energy consumption.

Design considerations for the integration of energy harvesting systems with energy-aware task schedulers

Leonardo Kessler Slongo, Arliones Hoeller Jr, Antônio Augusto Fröhlich, and Eduardo Augusto Bezerra

Figure 1

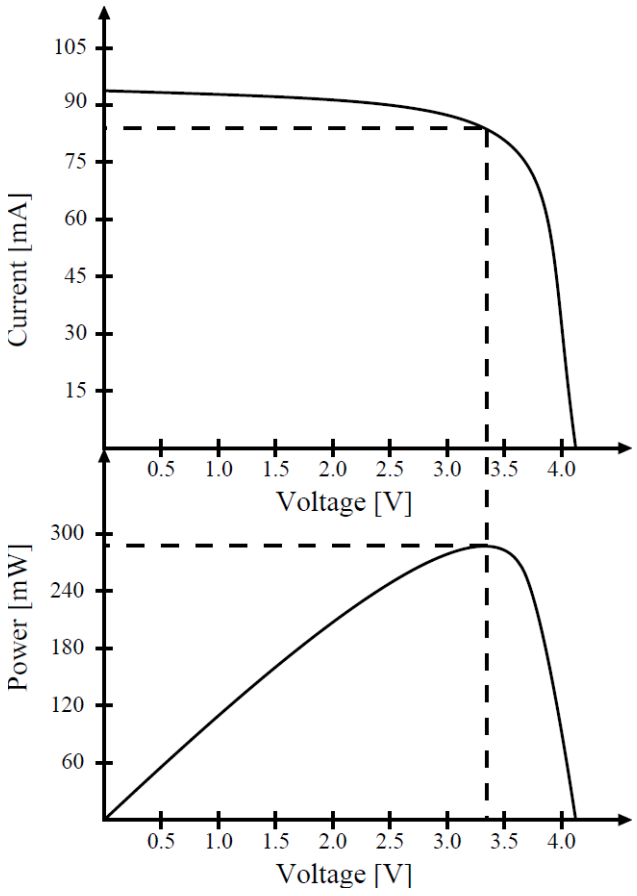

Design considerations for the integration of energy harvesting systems with energy-aware task schedulers

Leonardo Kessler Slongo, Arliones Hoeller Jr, Antônio Augusto Fröhlich, and Eduardo Augusto Bezerra

Figure 2

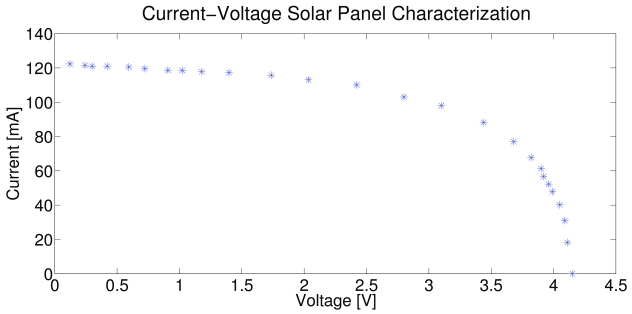

Design considerations for the integration of energy harvesting systems with energy-aware task schedulers

Leonardo Kessler Slongo, Arliones Hoeller Jr, Antônio Augusto Fröhlich, and Eduardo Augusto Bezerra

Figure 3

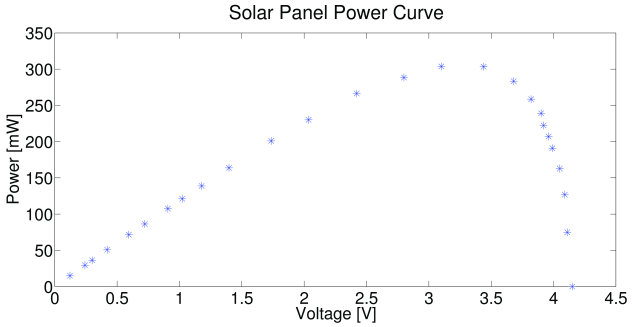

Design considerations for the integration of energy harvesting systems with energy-aware task schedulers

Leonardo Kessler Slongo, Arliones Hoeller Jr, Antônio Augusto Fröhlich, and Eduardo Augusto Bezerra

Figure 4

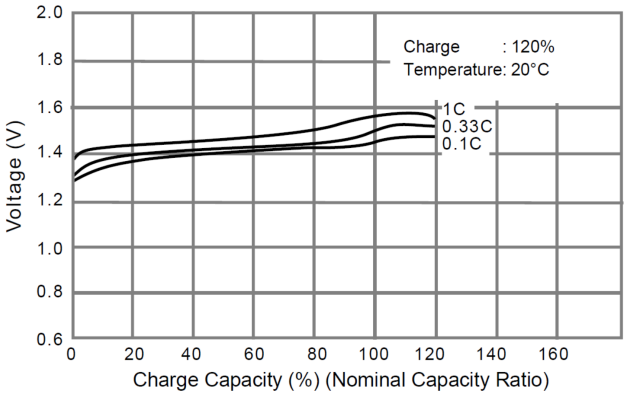

Design considerations for the integration of energy harvesting systems with energy-aware task schedulers

Leonardo Kessler Slongo, Arliones Hoeller Jr, Antônio Augusto Fröhlich, and Eduardo Augusto Bezerra

Figure 5

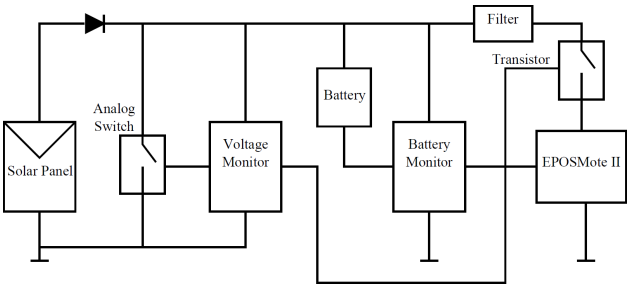

Design considerations for the integration of energy harvesting systems with energy-aware task schedulers

Leonardo Kessler Slongo, Arliones Hoeller Jr, Antônio Augusto Fröhlich, and Eduardo Augusto Bezerra

Figure 6

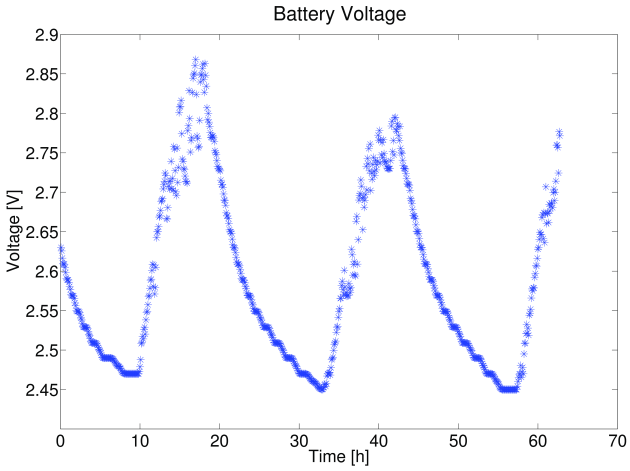

Design considerations for the integration of energy harvesting systems with energy-aware task schedulers

Leonardo Kessler Slongo, Arliones Hoeller Jr, Antônio Augusto Fröhlich, and Eduardo Augusto Bezerra

Figure 7

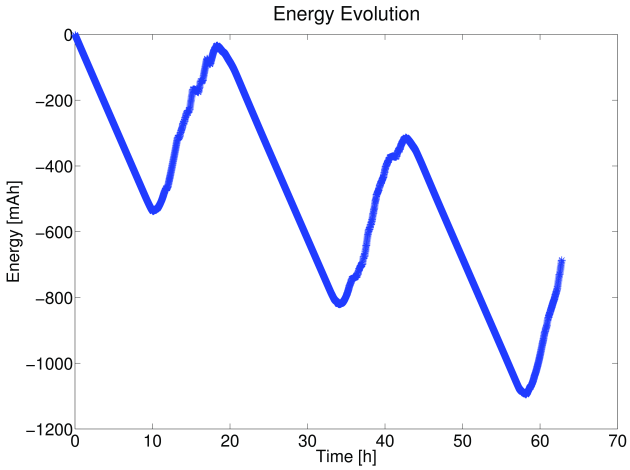

Design considerations for the integration of energy harvesting systems with energy-aware task schedulers

Leonardo Kessler Slongo, Arliones Hoeller Jr, Antônio Augusto Fröhlich, and Eduardo Augusto Bezerra

Figure 8

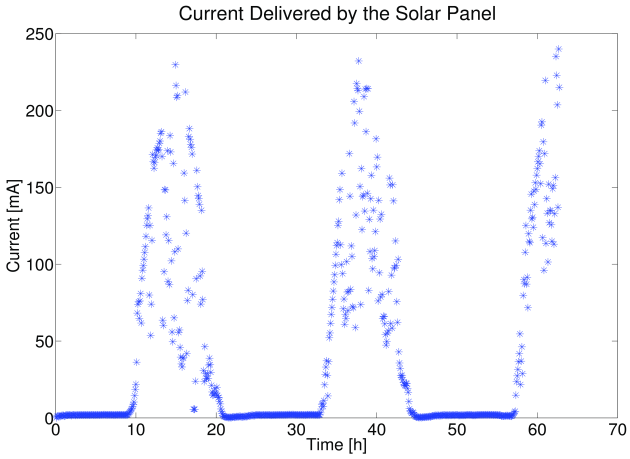

Design considerations for the integration of energy harvesting systems with energy-aware task schedulers

Leonardo Kessler Slongo, Arliones Hoeller Jr, Antônio Augusto Fröhlich, and Eduardo Augusto Bezerra

Figure 9

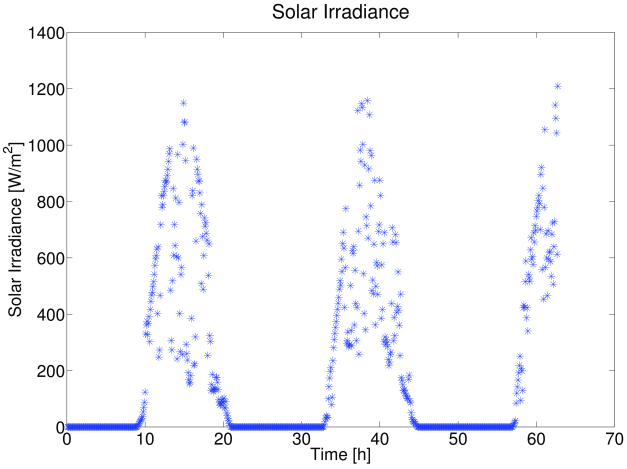

Design considerations for the integration of energy harvesting systems with energy-aware task schedulers

Leonardo Kessler Slongo, Arliones Hoeller Jr, Antônio Augusto Fröhlich, and Eduardo Augusto Bezerra

Figure 10

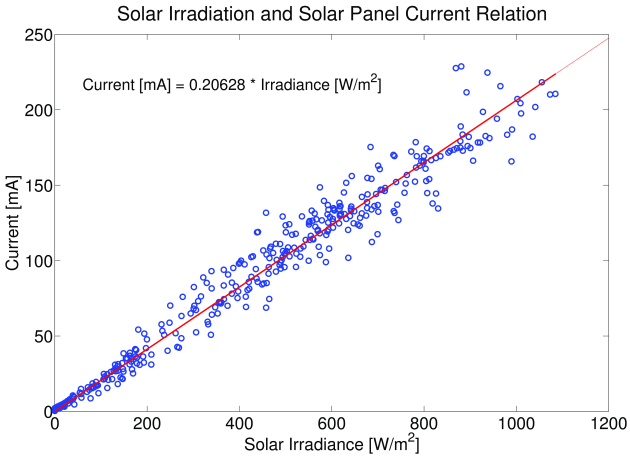

Design considerations for the integration of energy harvesting systems with energy-aware task schedulers

Leonardo Kessler Slongo, Arliones Hoeller Jr, Antônio Augusto Fröhlich, and Eduardo Augusto Bezerra

Figure 11

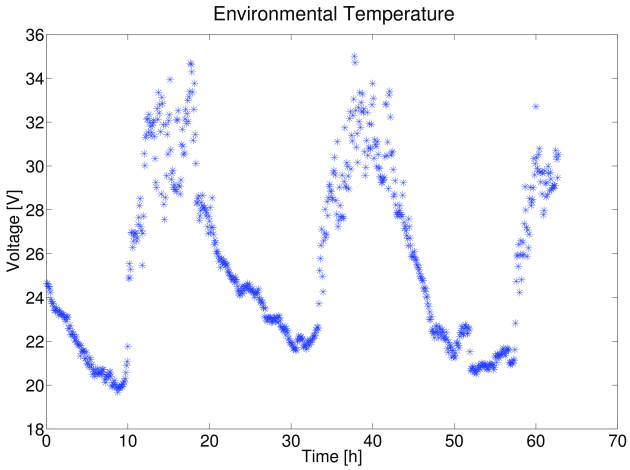

Design considerations for the integration of energy harvesting systems with energy-aware task schedulers

Leonardo Kessler Slongo, Arliones Hoeller Jr, Antônio Augusto Fröhlich, and Eduardo Augusto Bezerra

Figure 12

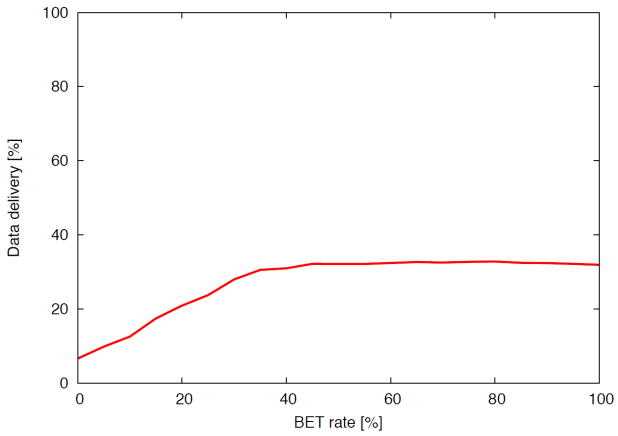

Design considerations for the integration of energy harvesting systems with energy-aware task schedulers

Leonardo Kessler Slongo, Arliones Hoeller Jr, Antônio Augusto Fröhlich, and Eduardo Augusto Bezerra

Figure 13

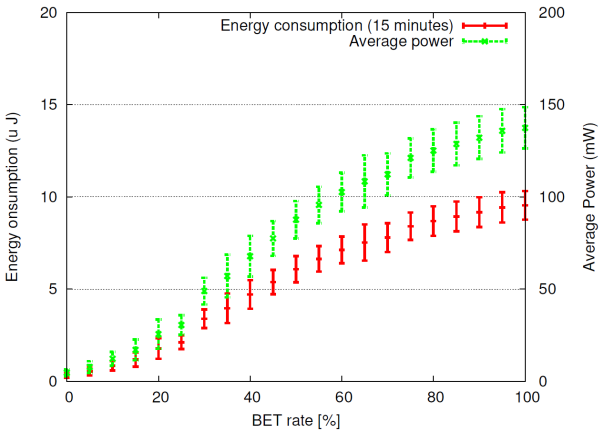

Design considerations for the integration of energy harvesting systems with energy-aware task schedulers

Leonardo Kessler Slongo, Arliones Hoeller Jr, Antônio Augusto Fröhlich, and Eduardo Augusto Bezerra

Figure 14

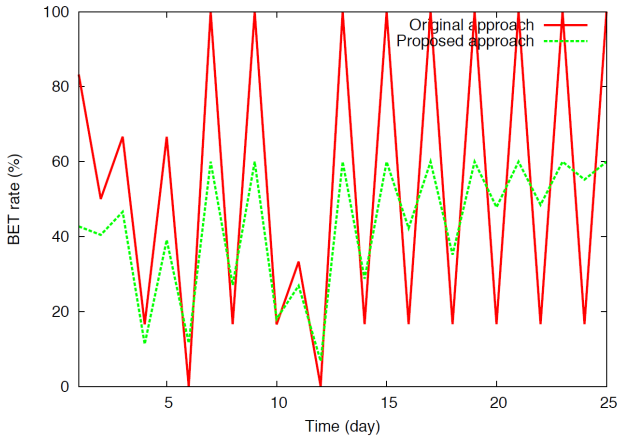

Design considerations for the integration of energy harvesting systems with energy-aware task schedulers

Leonardo Kessler Slongo, Arliones Hoeller Jr, Antônio Augusto Fröhlich, and Eduardo Augusto Bezerra

Figure 15